Propagation of magnetostatic waves in yttrium iron garnet films of submicron thickness

A. S. Andreev, Yu. V. Gulyaev, P. E. Zil'berman, V. B. Kravchenko, A. V. Lugovskoĭ, Yu. F. Ogrin, A. G. Temiryazev, and L. M. Filimonova

Institute of Radio Engineering and Electronics, USSR Academy of Sciences
(Submitted 4 July 1983)
Zh. Eksp. Fiz. **86**, 1005–1015 (March 1984)

High-grade submicron (thickness a $\lesssim 1\,\mu$m) epitaxial yttrium iron garnet films were obtained, and the propagation of magnetostatic waves (MSW) and MSW pulses in such films were investigated for the first time ever. Forbidden sections ("gaps"), in which no MSW are excited and do not propagate, were observed within the MSW spectrum. At a fixed frequency ($\sim$4 GHz) the magnetic-field widths in these gaps are $\sim$4–10 Oe, corresponding to frequency bands $\sim$10–30 MHz. The gap widths were found to be strongly anisotropic, i.e., dependent on the MSW propagation direction. With increasing film thickness, the gaps in the dispersion law decreases, collapse, and are transformed into anomalous-dispersion sections. The MSW pulses undergo strong dispersive distortions near the gap frequencies. A theory developed shows that the interaction of dipole and exchange waves can indeed produce in submicron films forbidden frequency bands. Comparison of this theory with experiment permits a qualitative, and in some cases also a quantitative explanation of the observations. In particular, it becomes possible to determine the constants that characterize the pinning of the spins to the free film surface and to the surface adjacent to the substrate.

Among the ferromagnets with narrow resonance lines (EuO, $CdCr_2Se_4$, $Y_3Fe_5O_{12}$, and others), epitaxial films of yttrium iron garnets (YIG) occupy a special place. They can be easily obtained as homogeneous, with large diameter, with various thicknesses $a = 0.1$–$40\,\mu$m, and most importantly, with as yet unprecedently narrow lines. In the better samples at room temperature, the homogeneous-resonance line reaches[1] $2\Delta H_0 \sim 0.15$ Oe. Such films serve as good media for the propagation of traveling magnetostatic waves (MSW). Up to now, MSW were investigated in films of rather large thickness, $a \gtrsim 3\,\mu$m (Refs. 1–5). Yet it is known that with decreasing thickness of the influence of the exchange energy on the MSW properties should become ever more strongly pronounced.[5–9] We deemed it natural and most interesting to investigate the manifestations of exchange effects in films having the minimum attainable thickness, submicron films, something apparently not performed before. The present paper is devoted just to the solution of this problem. We have grown submicron YIG films of good quality ($2\Delta H_0 < 0.5$ Oe) and investigated experimentally the propagation of MSW in such films in the cw and pulsed regimes. Moreover, we developed a theory with the aid of which we succeeded in explaining the observations qualitatively, and in some cases also quantitatively.

We investigated in the present study a wave of the Damon-Eshbach type[10] traveling in a tangential saturating external field $\mathbf{H}_0$ with a wave vector $\mathbf{q} \perp \mathbf{H}_0$. This wave is the most convenient for the investigation since, first, it is an isolated branch of the spectrum and, second, is sensitive to the influence of exchange interaction. It was indicated earlier[11] that such a dipole wave, since exchange boundary conditions must be satisfied on the film surface, must radiate spin waves into the interior of the film. The latter waves propagate in the film (as in a waveguide) in synchronism with the dipole wave that emits them, i.e., they have the same frequency ω and the same longitudinal vector $\mathbf{q}$. If the frequency ω approaches one of the film's spin-wave-resonance (SWR) frequencies ω_n ($n = 0, 1, 2\ldots$ is the number of the resonance),[12] the amplitudes of the spin (exchange) and dipole waves become comparable and a hybrid dipole-exchange wave is produced with singularities of the "anomalous" dispersion type[13] in the dispersion law. Such singularities were observed experimentally in Ref. 5 for a film with $a = 3.5\,\mu$m. In our experiments we also obtained anomalous-dispersion sections for films with $a \gtrsim 1.5\,\mu$m. In submicron films, however, we observed, rather than anomalous-dispersion sections, bands in which the MSW were totally blocked, or "gaps" in the spectrum. These gaps turned out to be large, of the order of 10–30 MHz, i.e., they constituted an appreciable part of the entire width of the spectrum. We investigated the dependence of the widths of the observed gaps on the film thickness and revealed the strong influence exerted on them by such factors as the crystallographic orientation of the substrate and of the orientation of the vector $\mathbf{q}$ in the film plane (anisotropy of the gaps). We investigated for the first time ever the propagation of MSW at frequencies adjacent to the gap. In this case we observed a rather strong dispersive distortion of the pulse waveform, a strong damping of their intensity at frequencies in the region of the gap, an appreciable increase of the delay time, and the appearance of several delayed "echo pulses."

A feature of submicron YIG films is satisfaction of the condition

$$a^2 \ll 4\alpha M_0/\Delta H_q, \tag{1}$$

where α is the inhomogeneous exchange constant ($\alpha = 3.3\times 10^{-11}$ cm^2), M_0 is the saturation magnetization ($M_0 \times 140$ G, and ΔH_q is the wave-damping parameter (half-width of the corresponding resonance). At $2\Delta H_q = 0.5$ Oe, for example, the condition (1) is satisfied if $a \ll 2.7\,\mu$m. We develop in this article a theory which shows that when (1) is

 0038-5646/84/030586-06$04.00

satisfied the spectrum of the hybrid dipole-exchange waves contains in the vicinity of ω_n frequency bands in which the MSW are freely transmitted. The spectrum spans a large interval of wave numbers q, and the width of this interval depends substantially on ΔH_q. No such spectrum was obtained in the known theories.[6–9,13] We have thus obtained a more accurate form of the MSW spectrum in submicron films.

1. EXPERIMENT

YIG films 0.5–1.5 μm thick were previously (e.g., Ref. 14) obtained on the gadolinium-gallium garnet $Gd_3Ga_5O_{12}$ (GGG) by the rocking-vessel method at an initial growth temperature 1000–1100 °C and using lead borate as the solvent. A number of studies, e.g., Refs. 15 and 16, were made of the conditions for obtaining YIG films with minimum ferromagnetic resonance (FMR) width, namely: maximum purity of the initial reagents, high growth temperature, low degree of supersaturation (which ensures a minimum Pb content in the film when lead-containing solvents are used), and good substrate quality. In accord with these data, we have grown the YIG films by the procedure of Ref. 16 on horizontal substrates of GGG single crystals with orientation (110) and (111). The solvent was $PbO–B_2O_3$. The substrate was rotated at 90 rpm, the film rate was 0.2–0.8 μm/min, $T_{\text{growth}} \approx 950$ °C, $\Delta T = T_{\text{sat}} - T_{\text{growth}} \approx 3–5$ °C, and the resultant film thicknesses were 0.2–5 μm. The width of the FMR lines at 9.3 GHz was less than 0.5 Oe. The unit-cell parameter for films grown at rates < 0.4 μm/min was 12.376 ± 0.003 Å, which corresponds practically to pure YIG. The width obtained with an x-ray diffractometer with a monochromator, for the diffraction lines $(880)\alpha_1$ of films with (110) orientation and (888) α_1 of films with (111) orientations, was $(0.3–1)'$, attesting to the high structural perfection of the films. No broadening or splitting of the diffraction maxima, which might be attributed to the possible presence[15] of transition layers on the film–substrate interface, was observed at all for the YIG films.

Rectangular samples with representative dimensions 10×5 mm were cut from the obtained films. These samples were placed on two aluminum microstrips of length 5 mm, width 5–6 μm, thickness 2 μm deposited by photolithography on the surface of a glass plate whose opposite side was clamped to a grounded metal plate. The distance between the strips was $l = 0.5$ mm. One of the strips was connected to a microwave oscillator and served as a transmitting antenna, and the other to a microwave receiver. The measurements were made at frequencies close to 4 GHz. The external field produced by an electromagnet was parallel to the strips.

Figure 1 shows the receiver input signal, with the field H_0 swept, as photographed from the scope screen. In a definite range of H_0 in which the wave of the investigated type exists, oscillations of this signal were observed. They are due to interference between the MSW signal and electromagnetic noise, both incident on the receiving antenna. In fact, the period of the oscillations agrees in magnitude and in H_0 dependence with the calculated interval between the interference maxima

$$\delta H_0 = (2\pi/l) \, |dq/dH_0|^{-1}$$

a similar interference was observed also earlier in films of relatively large thickness.[17] The distinguishing feature of the submicron films is the appearance of sections where the oscillations fade (Fig. 1). We believe that the fading is due to the cessation of MSW propagation (to the appearance of gaps) in those fields H_0 whose working frequency ω is close to one of the SWR frequencies ω_n. The latter can be verified by considering the dependences of the fields H_{0n}, taken at the center of each section, on the number n of this section. We assign the smallest number ($n = 0$) to the section at the maximum H_0. In Fig. 2 the experimental points yield the values of H_{0n} for different n. The straight lines are the calculated dependences of the resonant SWR fields on n^2. It can be seen that at equal thicknesses a the dependences of the resonance fields and of the fields H_{0n} on n^2 are close to one another.

Comparing the interference patterns in Figs. 1a and b, we see that the number of fading sections (gaps) within the limits of the MSW spectrum increases with increasing film

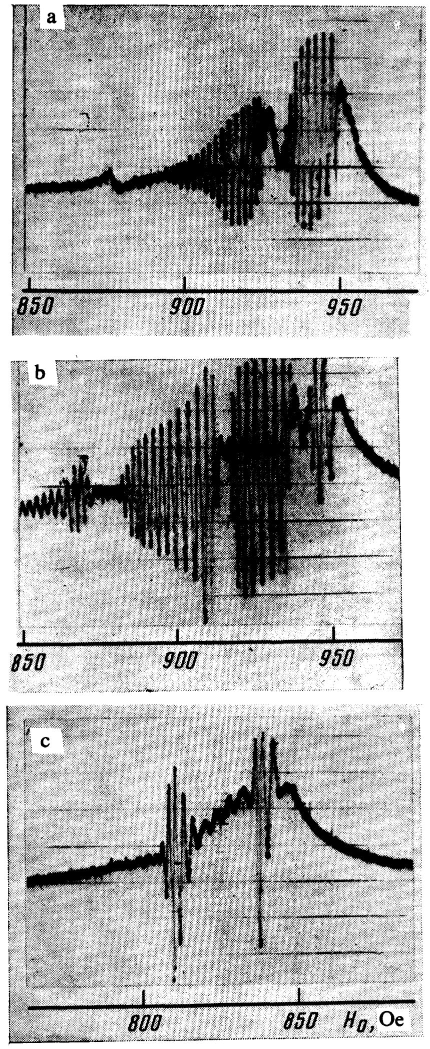

FIG. 1. Dependence of the receiver signal on the field H_0 (interference patterns): a—film with $a = 0.54$ μm on a (110) substrate $H_0 \| [100]$; b—film with $a = 0.81$ μm on a (110) substrate, $H_0 \| [100]$; c—film with $a = 0.8$ μm on a (111) substrate. MSW frequency $\omega/2\pi = 4310$ MHz.

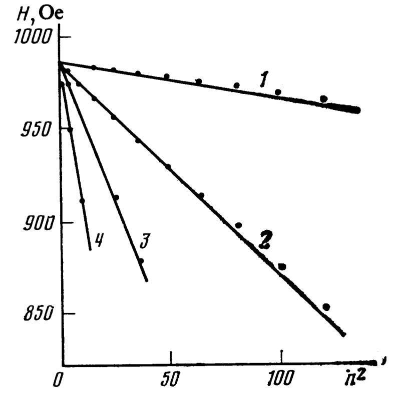

FIG. 2. Dependence of the resonant SWR fields (solid lines) and of the fields H_{0n} at the centers of the gaps (experimental points) on the number n of the gaps: 1—$a = 4.76\,\mu$m, 2—1.96, 3—1.22, 4—0.81.

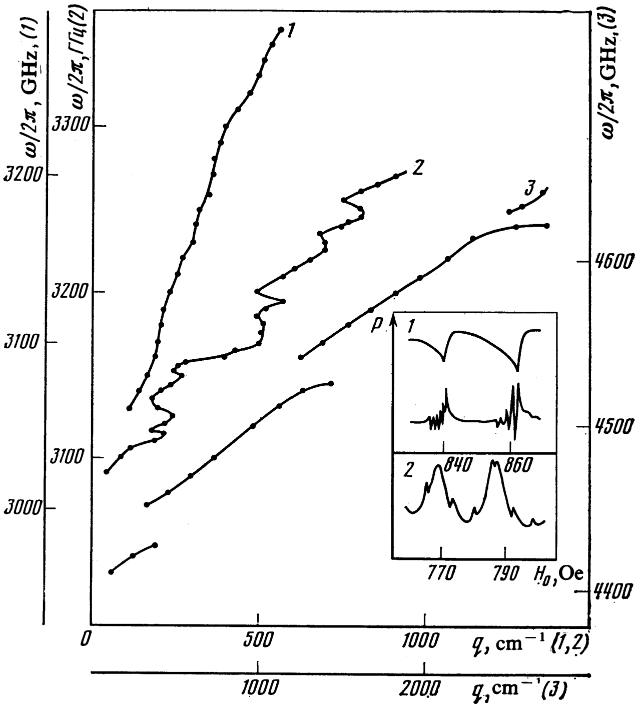

FIG. 4. Film dispersion laws: 1—$a = 4\,\mu$m, 2—1.55, 3—0.81. in the insets: 1) lower curve—interference pattern for film with $0.54\,\mu$m, upper—power reflected from transmitting antenna; 2) interference pattern for film with $a = 4.76\,\mu$m. Distance between antennas ≈ 2 mm, antenna width $\approx 20\,\mu$m.

thickness, and the widths of the gaps decrease somewhat. These tendencies are particularly clearly seen for large thickness changes, as for example on the interference patterns shown in the inset of Fig. 4 below. The widths of the gaps and their number depend substantially also on the crystallographic orientation of the substrate. It is seen from Figs. 1b and 1c that at a constant thickness, but on going from a substrate with developed plane (110) to a substrate with (111) plane, the gaps increase in width and decrease in number. This attests to anisotropy of the dispersion properties of the dipole and exchange MSW. Inside the gap, the noise signal varies nonmonotonically with H_0. The change of the noise is apparently a reflection of the dependence of the input impedance of the transmitting antenna on H_0.

Rotating the film sample placed on the antenna and observing the interference pattern at different rotation angles we note that the gap widths depend strongly on the angle. This dependence duplicates the angular dependence of the resonant FMR field. For example, the dependence for films on (110) substrate is similar to that shown in Gurevich's book[18] (Fig. 2.28, p. 95). The absolute maximum of the gap width is reached at $\mathbf{H}_0 \| [110]$, the minimum, equal to zero, at $\mathbf{H}_0 \| [111]$, while at $\mathbf{H}_0 \| [100]$ we have a certain local maximum. The foregoing illustrates the interference patterns of Fig. 1a and Figs. 3a and 3b, obtained for different orientations of a film with $a = 0.54\,\mu$m. For the same film ($a = 0.54\,\mu$m (110)), the inset of Fig. 4 shows above the interference pattern the measured H_0-dependence of the power reflected from the transmitting antenna. It is seen that at the center of the gap the power is a maximum and equal to the value outside the MSW spectrum. This shows directly that the gaps are due to cessation of the MSW excitation.

It is of interest to clarify the character of the variation of the MSW dispersion law near a gap as the film thickness is varied. Measurements of the dispersion law were made by the method of moveable receiving antenna,[5] the antenna being displaced at a low constant speed with an electric motor.[19] In these measurements we used thin antennas of $10\,\mu$m diameter. The results are shown in Fig. 4. At film thicknesses $\approx 4\,\mu$m the $\omega(q)$ dependence is practically monotonic. The influence of the dipole-exchange interaction manifests itself only in a weak waviness of $\omega(q)$. It is known[20] that for films of such thickness the exchange influences mainly the wave damping, which undergoes giant oscillations as a function of H_0 (or ω). When the film thickness is decreased to 1.55 μm the influence of the exchange on the dispersion law increases considerably—at frequencies near the resonant ω_n there appear clearly pronounced sections of nonmonotoni-

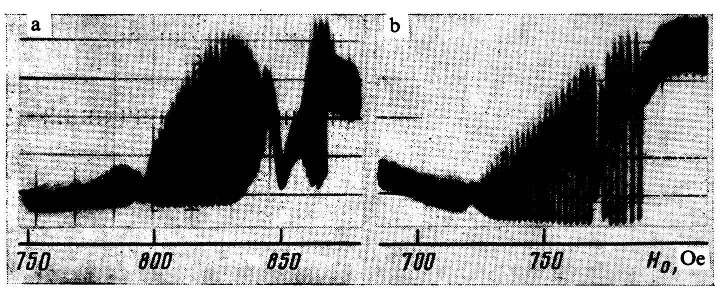

FIG. 3. Interference patterns for (110) film with $a = 0.54\,\mu$m at the frequency $\omega/2\pi = 4.148$ GHz; a—$\mathbf{H}_0 \| [110]$, b—$\mathbf{H}_0$ close in direction to [111].

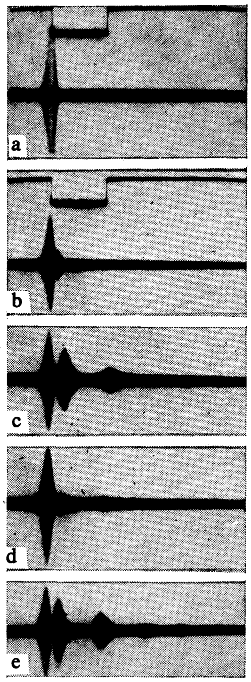

FIG. 5. Passage of MSW pulses. Film (110), $a = 0.81\,\mu$m, $H_0 \| [100]$. Frequency $\omega/2\pi = 4.310$ GHz, marker duration 0.5 μsec, $H_0 = 1044$ Oe (a), 955 Oe (b), 946 Oe (c), 942 Oe (d), 939 Oe (e).

city (of anomalous dispersion). Finally, at submicron thicknesses (0.81 μm) near the frequencies ω_n, frequency bands appear in which the MSW cannot be detected (gaps). We emphasize that in contrast to Ref. 5 we have observed quite broad MSW rejection bands (up to ≈ 10 MHz for a film with $a = 0.81$ and to ≈ 30 MHz for $a = 0.54\,\mu$m Fig. 1). In our experiments we measured the dispersion law up to values $q \approx 3\times 10^3$ cm.$^{-1}$

The presence of strong dispersion in the gap region should manifest itself in the propagation of MSW pulses. To observe this effect, the signal from the microwave oscillator (4.31 GHz) was modulated by pulses of duration $\tau_p \approx 0.2$ μsec at low repetition frequency and applied to the input of the setup to obtain the interference pattern of Fig. 1b. The received pulses were heterodyned to ≈ 160 MHz and displayed on an oscilloscope. Figures 5a–5e show these pulses at various H_0. Outside the MSW spectrum (Fig. 5a), only the noise pulse is observed. When the magnetic field is applied, a delayed MSW pulse appears—Figs. 5b. Further advance into the interior of the spectrum increases the delay time and causes noticeable spreading of the pulse—Fig. 5c. The most noticeable distortion of the MSW pulse shape is seen on Fig. 5d, where "corrugation" of the envelope of the delayed pulse is observed. It should be noted that Figs. 5c—5e show that not one but several delayed pulses arrive at the receiving antenna. One of the most probable causes of the appearance of such echo pulses is the excitation of magnetoacoustic waves in the film + substrate structure. This question, however, calls for a special study and is outside the scope of the present paper.

2. THEORY

We considered a model of an isotropic ferromagnetic layer in a tangential saturating field H_0, and MSW with a tangential vector $\mathbf{q}$–$\mathbf{H}$. The boundary conditions imposed on the layer surfaces were

$$\begin{aligned} &\frac{\partial \delta M_x}{\partial y} = 0, \quad \Lambda_1 \frac{\partial \delta M_y}{\partial y} - \delta M_y = 0 \quad \text{at} \quad y = a, \\ &\frac{\partial \delta M_x}{\partial y} = 0, \quad \Lambda_2 \frac{\partial \delta M_y}{\partial y} + \delta M_y = 0 \quad \text{at} \quad y = 0, \end{aligned} \tag{2}$$

where x and y are respectively the coordinates along the vector $\mathbf{q}$ and along the normal to the layer; $\delta\,\mathbf{M}$ is the vibrational component of the magnetization in the wave; $\Lambda_{1,2}$ are constants that describe the degree of spin pinning by the surfaces.[12] The following conditions were assumed satisfied:

$$\frac{q(\alpha/2\pi)^{1/2}}{[(1+\eta^2)^{1/2}-\eta_0]^{1/2}} \ll 1, \quad q|\Lambda_{1,2}| \ll 1, \quad \delta = \frac{2}{a}\left(\frac{\alpha}{2\pi}\right)^{1/2} \ll 1, \tag{3}$$

where $\eta = 2\omega/\omega_m$, $\omega_m = 4\pi\gamma M_0$, $\gamma > 0$ is the gyromagnetic ratio $\eta_0 = \eta_H + 1$, $\eta_H = 2\omega_H/\omega_m$, $\omega_H = \gamma H_0$. The conditions (3) denote relatie smallness of the exchange-energy contribution and sufficiently strong spin pinning. These conditions can be realistically satisfied in YIG at $a > 0.2\,\mu$m and not too close to the lower (in frequency) end point of the spectrum, when $(1+\eta^2)^{1/2} \neq \eta_0$. On the basis of the precession and magnetostatics equations, we obtained in standard fashion (see, e.g., Ref. 7) the following MSW dispersion equation:

$$\begin{aligned} &(T^2-R^2-S^2)\,[e^{qa}(\eta_0^2-\eta^2)-e^{-qa}] \\ &= 2q\left(\frac{\alpha}{2\pi}\right)^{1/2}[(\eta^2-\eta_H^2)(S+Te^{qa})-2\,\mathrm{sh}\,qa(T\eta_H+R\eta)], \\ &q \geqslant 0, \end{aligned} \tag{4}$$

where

$$T \pm R = \frac{\delta(p-1)(p+\eta_0)}{2p}\zeta\left(\mathrm{ctg}\,2\zeta + \frac{2\Lambda^*_{1,2}}{a}\zeta\right), \tag{5}$$

$$S = -\frac{\delta(p-1)(p+\eta_0)}{2p}\frac{\zeta}{\sin 2\zeta}, \tag{6}$$

$$\Lambda^*_{1,2} = \Lambda_{1,2}\frac{2p}{(p-1)} - \frac{1}{(p+\eta_0)^{1/2}}\left(\frac{\alpha}{2\pi}\right)^{1/2}\frac{(p+1)}{(p-1)}, \tag{7}$$

$$\zeta = \frac{(p-\eta_0)^{1/2}}{\delta}, \quad p = (1+\eta^2)^{1/2}. \tag{8}$$

The vanishing of the first factor in the left-hand side of (4) determines the SWR frequencies, and that of the second factor the dispersion law of the Damon-Eshbach dipole wave. The right-hand side describes the connection of the dipole and exchange fields.

We shall show that Eq. (4) leads to the conclusion that gaps exist near the SWR frequencies. This is easiest to do at $\Lambda_1 = \Lambda_2 \equiv \Lambda$, i.e., $R \equiv 0$. It is seen from (5) and (6) that in the vicinity of their zeros the frequency functions $T \pm S$ are decreasing ones, i.e., $T \pm S > 0$ at $\omega = \omega_n - \omega'$ and $T \pm S < 0$ at $\omega = \omega_n + \omega'$, where $\omega' \to +0$ and n is the number of the SWR mode. The right-hand side of (4) is non-negative in the vicinity of the SWR frequencies, as can be easily verified by substituting in it $T = \pm S$. We shall approach some SWR frequency from below ($\omega \to \omega_n - 0$). Then $T \pm S \to +0$. Equation (4) might be satisfied only as $q \to 0$ (we emphasize that, by definition, $q \geqslant 0$, and this was used basically in the derivation of (4)). If $q \to 0$, however, the quantity in the square brackets on the left in (4) is negative in the entire frequency range in which SWR exist (i.e., ζ is real or $\eta^2 \geqslant \eta_0^2 - 1$). Thus, the left- and right-hand sides of (4) have opposite signs and the equation cannot have any solutions as $\omega \to \omega_n - 0$. This proves in fact that existence in the frequency spectrum of a forbidden band (gap) whose bottom is equal to the SWR frequency.

The existence of such bands was not noted before. In Refs. 7 and 13 they investigated only a small vicinity of the intersection point of the dispersion curves of the dipole and exchange waves, and repulsion of these curves in this vicinity was obtained. A numerical analysis[6,9] yielded likewise no forbidden frequencies. To understand qualitatively the cause of the appearance of the gap, we note that the right-hand side of (4) (the coupling of the waves) increases with q in view of the presence of the factor $q\sqrt{\alpha}$. Therefore, although by increasing q we move away from the intersection point of the dispersion curves, the waves remain hybrid and the branches of the spectrum continue to be pushed apart. Of course, such a gap can collapse at very large q, at which (3) is violated, or in sufficiently strong dissipative processes. To discuss the role of these factors, we proceed to a more detailed description of the form of the dispersion law near the gap.

Let us describe the dispersion law at $\xi \equiv qa \ll 1$. We consider the case of strong surface pinning of the spins, at which $2|\Lambda^*_{1,2}|a \ll 1$. It is known[7,21] that in this case the dipole-exchange interaction is particularly effective. We shall see that the gap is in this case also a maximum. Linearizing (4) with respect to ξ, we get

$$\xi = \frac{(\eta^2+1-\eta_0^2)(T-S)}{[2(T-S)-\delta(\eta^2-\eta_H^2)]}. \tag{9}$$

It follows from (9) that the forbidden frequencies are obtained from the conditions

$$0 \leqslant (T-S) \leqslant {}^1/_2\delta(\eta^2-\eta_H^2), \tag{10}$$

since the solution must ensure satisfaction of the inequality $\xi \geqslant 0$.

The analysis on the basis of the complete Eq. (4) remains in force by virtue of the condition (10)–the lower limit of the gap can only be lowered somewhat at $\xi \gtrsim 1$. Using the definitions (5) and (6) and the conditions (3), we obtain from the equation $(T-S)=0$ the upper end point of the gap (the SWR frequency) in the form $\zeta_n \equiv \zeta(\omega_n) = n\pi/2$, where $n = 1, 3, 5, \cdots$. At this frequency the wave number of the dipole wave is

$$\xi = {}^1/_2(\eta^2+1-\eta_0^2) = \delta^2\zeta_n^2(\eta_0 + {}^1/_2\delta^2\zeta_n^2) \ll 1,$$

if $\delta^2\zeta_n^2\eta_0 \ll 1$. Since (3) is satisfied and $\eta_0 \gtrsim 1$, the last enhanced inequality can be satisfied, but only for the first numbers n. Satisfaction of this inequality is essential to be able to describe with the aid of (9) the region near and to the right of (relative to q) the synchronism point of the dipole and exchange waves. If it is recognized that $\delta^2\zeta_n^2\eta_0 \ll 1$ the lower end point of the gap is found from the equation $(T-S) = {}^{1/2}\delta(\eta^2 - \eta H^2)$ to be equal to 0 at $n = 1$ and to $\zeta_n - \zeta_n^{-1}$ at $n = 3, 5, \cdots$. Thus, th gap width is $\Delta\zeta_1 = \zeta_1$ and $\Delta\zeta_n = \zeta_n^{-1}$ at $n = 3, 5, \cdots$. In the original notation we obtain for the gap width $\omega_g(n)$

$$\omega_g(n) = \omega_m \frac{\alpha}{\pi a^2} \frac{(\omega_H+\omega_m/2)}{(\omega_H^2+\omega_H\omega_m)^{1/2}} \begin{cases} \pi^2/4, & n=1 \\ 2, & n=3,5,\ldots \end{cases} \tag{11}$$

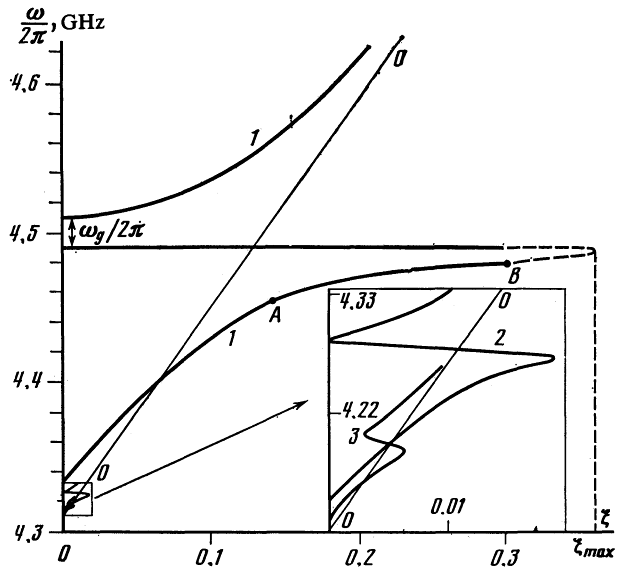

FIG. 6. Calculated form of dispersion law: 00—for dipole wave, 1—for hybrid exchange-dipole wave at $a = 0.81\ \mu$m, 2—the same at $a = 2.8\ \mu$m, 3—the same at $a = 4.0\ \mu$m. In all cases $2\Delta H_q = 0.5$ Oe and $H_0 = 888$ Oe. The inset shows the initial section of the spectrum in enlarged scale.

It can be seen from (11) that the gap width changes little with the number n, but on the other hand it increases with decreasing film thickness a (like a^{-2}) and is therefore particularly large in submicron films. Substituting the YIG parameters at $a = 1\ \mu$m we get $(\omega_g/2\pi) \sim 20$ MHz, in good agreement with experiment. The dissipative processes can be taken into account by making in (9) the substitution $H_0 \to H_0 - i\Delta H_q$. It turns out then that if (1) is satisfied the expressions (11) remain in force, and the dispersion law takes the form shown in Fig. 6 (curve 1). It can be seen that the spectrum of the hybrid waves covers a large interval of wave numbers up to

$$\xi_{max} \approx \eta_0\delta^2\zeta_n^2 \frac{4\alpha M_0}{a^2\,\Delta H_q} \gg \eta_0\delta^2\zeta_n^2,$$

and at $\xi = \xi_{\max}$ there is a vertical tangent and the dispersion curve begins to return to small ξ. As already noted, in submicron films the condition (1) is satisfied with good margin. Therefore the dispersion properties of MSW in such films are not very sensitive to the film quality (so long as $2\Delta H_q < 5$ Oe). At the same time these properties depend strongly on the thickness a. A small increase of the thickness leads to collapse of the gap, so that only the section of anomalous dispersion remains—Fig. 6, curves 2 and 3.

Let us discuss also the question of the consequences of violation of the first condition of (3). It is violated $\xi \gtrsim 2\zeta_n \geqslant \pi$, meaning $q \gtrsim \pi/a > 3.10^4\ \text{cm}^{-1}$ for $a < 1\ \mu$m. Such large q are not excited in practice and are not received by the microstrip antennas used in the MSW technique.[3] Therefore, although in principle purely exchange waves could propagate for such q even inside the gap described by us, they do not occur at all in experiment.

3. DISCUSSION

Let us consider in greater detail the correspondence between the reported experimental results and the theory. In a real film structure one cannot expect identical spin pinning on the free film surface and on the one in contact with the substrate, i.e., $\Lambda_1 \neq \Lambda_2$. In addition, the pinning may not be strong enough to be able to assume that $(2\Lambda^*_{1,2}/a) \to 0$. We therefore return to Eq. (4) and assume only one simplification, viz., $\xi \ll 1$. We can then solve (4) for ξ, and obtain

$$\xi = \frac{(\eta^2+1-\eta_0^2)(T^2-R^2-S^2)}{[2(T^2-R^2-S^2)-\delta^2(\eta^2-\eta_H^2)(T+S)]} \tag{12}$$

as $R \to 0$ (i.e., $\Lambda_1 \to \Lambda_2$), Eq. (12) goes over into (9), and an entire series of SWR, the one obtained from the equation $T+S=0$, is lost. The reason is the existence at $\Lambda_1 = \Lambda_2$ of a symmetry plane in the film, the ensuing lower efficiency of excitation of modes from this series by the almost uniform ($\xi \ll 1$) field of the dipole wave. Allowance for terms $\sim \xi^2$ in (9) allows us to estimate the sizes of the gaps near the frequencies of the "lost" series–they turn out to be smaller by a factor ξ than the ones obtained from (11). The situation is entirely different at $\Lambda^1 \neq \Lambda^2$ (i.e., at $R \neq 0$). Since there is no symmetry plane in this case, all the SWR sets are effectively excited by dipole waves. Therefore, when numbering the SWR modes (and meaning also the gaps) we shall refer the odd numbers n, as before, to the sets excited at $\Lambda_1 = \Lambda_2$, and the odd ones to the sets excited only at $\Lambda_1 \neq \Lambda_2$. The upper end point of the gap (or the SWR frequency), ω_n, is obtained from the condition that the numerator of (12) vanish; this yields the equation

$$\zeta_n \operatorname{ctg} 2\zeta_n = \frac{a}{2(\Lambda_1^*+\Lambda_2^*)}\left[1-\zeta_n^2\frac{4\Lambda_1^*\Lambda_2^*}{a^2}\right], \quad n=0,1,2,\ldots, \tag{13}$$

in which $\zeta_n \equiv \zeta(\omega_n)$. The lower end point ω_n^* of the gap is obtained from the condition that the denominator of (12) vanish, which yields

$$\left(\frac{\operatorname{tg}\zeta_n^*}{\zeta_n^*}-1\right)-\frac{(\Lambda_1^*+\Lambda_2^*)}{a}+\zeta_n^{*2}\frac{4(\Lambda_1^*\Lambda_2^*)}{a^2} + \zeta_n^* \operatorname{ctg} 2\zeta_n^* \frac{2(\Lambda_1^*+\Lambda_2^*)}{a}=0, \tag{14}$$

where $\zeta_n^* \equiv \zeta(\omega_n^*)$ and it is assumed that $\eta_0\delta^2\zeta_n^2 \ll 1$. A graphic analysis of the equations (13) and (14) shows that the gap widths determined from them (independently of the sign of $\Lambda^*_{1,2}$) are smaller than the values as $(2\Lambda^*_{1,2}/a) \to 0$. We use now (13) and (14) to analyze the interference patterns of Fig. 1b. Four gaps can be seen at $n = 0, 1, 3$, and . The frequency is fixed and equal to 4.31 GHz. The left end-point of the nth gap determines ζ_n, and the right ζ^*_n. To determine $2\Lambda^*_1/a$ and $2\Lambda^*_2/a$ we can make up from (13) and (14) four pairs of independent quadratic equations. We then verify directly that all these equations pairs are satisfied by the values $\Lambda_1^* = -3.24 \cdot 10^{-5}$ cm, which corresponds to $\Lambda_1 = -7.20^{-6}$ cm and $\Lambda_2 = -10^{-6}$ cm. Thus, Eqs. (13) and (14) are indeed valid for the interpretation of the interference patterns and enable us to find the constants of the surface pinning of the spins. The spin pinning is very strongly asymmetric. On one of the surfaces (apparently the one in contact with the substrate) the spins are practically completely pinned. The experimentally observed anisotropy of the gap widths is most probably due to anisotropy of the spin pinning, i.e., of the parameters $\Lambda^*_{1,2}$. The anisotropy of the dissipative parameter ΔH_q makes no contributions, inasmuch as under real conditions the gap width does not depend at all on ΔH_q.

The calculated form of the dispersion law (Fig. 6, curves 1 and 2) helps understand qualitatively also certain observed peculiarities of the propagation of the pulses, Fig. 5. For example, an increase of the delay time and the spreading of the delayed pulses on Fig. 5c are connected with landing in the region of large curvature–point A on curve 1 of Fig. 6. The drastic weakening of the delayed pulses on Fig. 5d is due to the influence of the gap. The gap is incapable of total extinction of the pulses, since the pulse occupies a frequency band $1/\tau_p$ comparable with the gap width. The corrugation of the delayed pulses in Fig. 5d is apparently due to the inflection of curve 1 at the point B (Fig. 6), as was indeed predicted by the theory.[22]

[1] J. D. Adam and J. H. Collins, Proc. IEEE **64**, 794 (1976).
[2] Yu. V. Gulyaev and P. E. Zil'berman, Radiotekh. Elektron. **23**, 794 (1978).
[3] F. I. Shekhtman, Rad. za rubezhom (Radio Engg. Abroad), No. 25, pp. 5-22.
[4] D. D. Adam, M. R. Daniel, and D. C. Schroder, Electronics [Russ. Transl.] **53**, 11 (1980)].
[5] W. Schilz, Philips Res. Repts. **28**, 50 (1973).
[6] R. E. de Wames and T. Wolfram, J. Appl. Phys. **41**, 987 (1970).
[7] B. N. Filippov, Fiz. Met. Metallov. **35**, 28 (1978). Preprint, Inst. Met. Phys. Ural Scient. Center, USSR Acad. Sci. No. 80/1, Sverdlovsk, 1980.
[8] R. G. Khlebopros and L. V. Mikhaĭlovskaya, Izv. AN SSSR, ser. fiz. **36**, 1522 (1972).
[9] B. A. Kalinikos, Izv. Vyssh. Ucheb. Zav. Fizika **24**, No. 8,42 (1981).
[10] R. W. Damon and J. R. Eshbach, J. Phys. Chem. Soc. **19**, 308 (1961).
[12] N. M. Salanskiĭ and M. Sh. Erukhimov, Physical Properties of Magnetic Films [in Russian] Nauka, Novosibirsk, 1975, p. 40.
[13] A. V. Logovskoĭ and P. E. Zil'berman, Fiz. Tverd. Tela (Leningrad) **24**, 458 (1982) [Sov. Phys. Solid State **24**, 259 (1982)].
[14] R. C. Linares, J. Crystal Growth **34**, 443 (1968).
[15] J. M. Robertson, M. J. J. van Hout, J. C. Verplanke, and J. C. Brice, Materials Research Bull. **9**, 555 (1974).
[16] H. L. Glass and M. T. Elliot, J. Cryst. Growth **36**, 285 (1976).
[17] S. A. Borisov, G. M. Novikov, and A. V. Stal'makhov, Proc. 5th Internat. Conf. on Gyromagnetic Electronics and Electrodynamics [in Russian], Moscow, 1980, Vol. 4, p. 26.
[18] A. G. Gurevich, Magnetic Resonance in Ferrites and Antiferromagnets [in Russian], Nauka 1973.
[19] Yu. V. Ogrin, A. V. Lugovskoĭ, and A. G. Temiryazev, Abstracts, 8th All-Union School-Seminar, "New Magnetic Materials for Micro-electronics,"Donetsk, 1982, p. 292.
[20] Yu. V. Gulyaev, A. S. Bugaev, P. A. Zil'berman *et al.* Pisma Zh. Eksp. Teor. Fiz. **30**, 600 (1979) [JETP Lett. **30**, 565 (1979)].
[21] I. A. Gilinskiĭ and K. A. Ryazantsev, Abstracts, 10th All-Union Conf. on Magnetism, Krasnoyarsk, 1971, p. 177.
[22] L. A. Vaĭnshtein, Usp. Fiz. Nauk **118**, 346 (1976) [Sov. Phys. USP. **19**, 189 (1976)].

Translated by J. G. Adashko